Chemistry of a Cofacial Dirhodium Diporphyrin: Synthesis and Reactivity of Rh_2DPB

James P. Collman,*,† Yunkyoung Ha,† Roger Guilard,‡ and Michel-Angel Lopez‡

Department of Chemistry, Stanford University, Stanford, California 94305

Received September 10, 1992

A novel cofacial dirhodium diporphyrin with a metal–metal single bond has been synthesized in two steps from the corresponding free base cofacial porphyrin H_4DPB. Rhodium insertion and subsequent photolysis yield the cofacial dirhodium diporphyrin Rh_2DPB. This cofacial dirhodium diporphyrin activates H_2 with the assistance of ancillary ligands which attack the rhodium centers externally, weakening the metal–metal bond. The reaction of the dirhodium diporphyrin with H_2 and CO yields the dirhodium diporphyrin dihydride Rh(H)Rh(H)DPB. The H_2 cleavage reaction seems to occur within the cavity of the cofacial diporphyrin, on the basis of the unusually high T_1 values of the resultant hydrides and the predicted regiospecific bonding pattern of additional, bulky ancillary ligands. This reactivity differs from that of a monomeric rhodium porphyrin system which gives a formyl complex. Phosphines have also been employed in reaction with the dirhodium diporphyrin and H_2, resulting in a different type of hydride complex, seemingly one having three-center two-electron bonds.

Introduction

Rhodium porphyrins have been of great interest for several reasons: Rhodium porphyrins containing functional groups have been used to mimic biological molecular recognition.[1] Organic substrates undergo redox transformations with rhodium porphyrins.[2] Methane activation has been achieved with rhodium porphyrin radicals.[3]

Wayland et al. studied CO and H_2 activation by rhodium porphyrins and synthesized a rhodium formyl porphyrin complex by the formal insertion of CO into a metal–hydride (M–H) bond.[4] This species is a potential intermediate in transition metal catalyzed reactions using CO and H_2. Wayland then carried out methane activation using Rh(TMP)• (TMP = tetra-*meso*-mesitylporphyrin) and determined that the reaction rate is second order in Rh(TMP)• and first order in CH_4.[3] He postulated a trimolecular transition state with a linear four-centered array involving a C–H bond bound between two rhodium centers. Both formyl group formation and CH_4 activation processes depend upon the unusually high Rh–C bond energy (ca. 57–58 kcal/mol) manifested by organorhodium porphyrin complexes[5] and the tendency of Rh(II) porphyrins to undergo free-radical reactions.[6]

We sought to emulate such small-molecule activation with cofacial Rh(II) porphyrins. This paper details the synthesis of a cofacial dirhodium(II) diporphyrin, Rh_2DPB (Figure 1), and its reactivity with H_2 in the presence of ancillary ligands. The reaction of Rh_2DPB with H_2 in the presence of CO yields a result different from that of monomeric porphyrins. Unusually large T_1 values are exhibited by the resulting dimeric hydrides in contrast to the extremely small T_1 values found in the monomeric system. These different reactivities and properties can be explained by contrasting the open face of a monomeric porphyrin with the crowded inner cavity of a cofacial diporphyrin. In contrast to the reaction of Rh_2DPB with H_2 in the presence of CO, the use of phosphines or phosphites as ancillary ligands in the reaction of Rh_2DPB with H_2 gives a different result. Tentative structures of the resulting hydrides are proposed on the basis of spectroscopic data.

Results and Discussion

Syntheses and Characterizations of Rhodium Insertion Products. Rhodium insertion into the diporphyrin H_4DPB is more challenging than in monomeric porphyrin systems. Several methods that yield monomeric Rh(III) porphyrins were attempted with the diporphyrin.[4b,7-9] In the case of the diporphyrin only one method yielded identifiable products with modest yields. The reaction of H_4DPB with $[Rh(CO)_2Cl]_2$ in $CHCl_3$ in the presence of anhydrous sodium acetate, followed by oxidation with I_2, produces three products (**1–3**) (eq 1). The rhodium insertion products, **1–3**, were characterized by IR, mass spectroscopy, ^1H NMR, and UV–vis.

$$H_4DPB + [Rh(CO)_2Cl]_2 \xrightarrow[CHCl_3]{NaOAc} \xrightarrow{I_2} Rh_2(I)_2DPB\ (\mathbf{1}) + Rh_2(CO_2Et)(I)DPB\ (\mathbf{2}) + Rh_2(CO_2Et)_2DPB\ (\mathbf{3}) \quad (1)$$

While the IR spectrum of **1** does not show carboxyl stretching bands, the spectra of metalloesters **2** and **3** confirm the presence of the expected carboxyl groups. The $\nu(C{=}O)$ of η^1-acyl organometallic compounds is usually found around 1650 cm^{-1},[10]

† Stanford University.

‡ Present address: Universite de Bourgogne, Laboratoire de Synthèse et d'Electrosynthèse Organométallique Associé au CNRS (UA 33), Faculté des Sciences "Gabriel", 21100 Dijon Cedex, France.

(1) (a) Aoyama, Y.; Yamagishi, A.; Tanaka, Y.; Toi, H.; Ogoshi, H. *J. Am. Chem. Soc.* **1987**, *109*, 4735–4737. (b) Aoyama, Y.; Yamagishi, A.; Asagawa, M.; Toi, H.; Ogoshi, H. *J. Am. Chem. Soc.* **1988**, *110*, 4076–4077. (c) Aoyama, Y.; Uzawa, T.; Saita, K.; Tanaka, Y.; Toi, H.; Ogoshi, H.; Okamoto, Y. *Tet. Lett.* **1988**, *29*, 5271–5274. (d) Aoyama, Y.; Nonaka, S.-I.; Motomura, T.; Ogoshi, H. *Chem. Lett.* **1989**, 1877–1880. (e) Aoyama, Y.; Motomura, T.; Ogoshi, H. *Angew. Chem., Int. Ed. Engl.* **1989**, *28*, 921–922. (f) Ogoshi, H.; Hatakeyama, H.; Yamamura, K.; Kuroda, Y. *Chem. Lett.* **1990**, 51–54. (g) Aoyama, Y.; Asakawa, M.; Yamagishi, A.; Toi, H.; Ogoshi, H. *J. Am. Chem. Soc.* **1990**, *112*, 3145–3151.

(2) (a) Aoyama, Y.; Fujisawa, T.; Watanabe, T.; Toi, H.; Ogoshi, H. *J. Am. Chem. Soc.* **1986**, *108*, 943–947. (b) Aoyama, Y.; Tanaka, Y.; Fujisawa, T.; Watanabe, T.; Toi, H.; Ogoshi, H. *J. Org. Chem.* **1987**, *52*, 2555–2559.

(3) (a) Sherry, A. E.; Wayland, B. B. *J. Am. Chem. Soc.* **1990**, *112*, 1259–1261. (b) Wayland, B. B.; Ba, S.; Sherry, A. E. *J. Am. Chem. Soc.* **1991**, *113*, 5305–5311.

(4) (a) Wayland, B. B.; Woods, B. A. *J. Chem. Soc., Chem. Commun.* **1981**, 700–701. (b) Farnos, M. D.; Woods, B. A.; Wayland, B. B. *J. Am. Chem. Soc.* **1986**, *108*, 3659–3663.

(5) Wayland, B. B. *Polyhedron* **1988**, *7*, 1545–1555.

(6) Paonessa, R. S.; Thomas, N. C.; Halpern, J. *J. Am. Chem. Soc.* **1985**, *107*, 4333–4335.

(7) Callot, H. J.; Schaeffer, E. *Nouv. J. Chim.* **1980**, *4*, 311–314.

(8) Ogoshi, H.; Setsune, J.-I.; Omura, T.; Yoshida, Z.-I. *J. Am. Chem. Soc.* **1975**, *97*, 6461–6466.

(9) Aoyama, Y.; Yoshida, T.; Sakurai, K.-I.; Ogoshi, H. *Oganometallics* **1986**, *5*, 168–173.

0020-1669/93/1332-1788$04.00/0

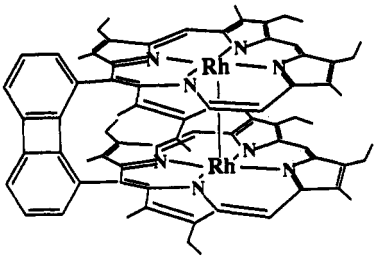

Figure 1. Rh_2DPB (DPB = Diporphyrinatobiphenylene).

and an (ethoxycarbonyl)rhodium etioporphyrin and its TPP (TPP = tetra-*meso*-phenylporphyrin) analog show ν(C=O) bands respectively at 1690 and 1700 cm^{-1}.[11,12] The C=O stretching frequencies in **2** and **3** also appear in these frequency ranges (ν(C=O) of **2** = 1691 cm^{-1}; ν(C=O) of **3** = 1687 cm^{-1}). In addition, the ν(C–O) bands of these metalloesters have been tentatively assigned (ν(C–O) of **2** = 1061 cm^{-1}; ν(C–O) of **3** = 1075 cm^{-1}). These values are typical for the C–O single bond stretch for ester groups (1000–1300 cm^{-1}).[13]

The molecular ion of **1** was not detected in mass spectroscopy; only m/e = 1307, which is equal to the mass of the Rh_2DPB fragment, is seen. There is no upfield signal above 0 ppm in the ^{1}H NMR spectrum of **1**, indicating that the axial ligands do not contain hydrogen atoms but are presumably iodides from the I_2 employed for the rhodium oxidation. Elemental analysis quantified the iodide present in **1**. Compound **2** was found to contain one iodide and one ethoxycarbonyl group as axial ligands. The origin of the ethoxy group is not obvious, but the small amount of ethanol present in chloroform as a stabilizer is likely the source of the axial ethoxycarbonyl group. Insertion of the Rh(I) carbonyl sitting-on-top complex into the porphyrin rings probably occurs by attack of ethanol on a carbonyl group in the rhodium complex to form an axially coordinated ethoxycarbonyl group. Compound **3** shows peaks of m/e = 1380 and 1307 in addition to a molecular ion of m/e = 1453. The difference of m/e = 73 between these peaks is due to the loss of one and two ethoxycarbonyl fragments.

The proton resonances of the axial ethoxycarbonyl groups appear upfield in the ^{1}H NMR because they experience an anisotropic diamagnetic shift resulting from the porphyrin ring current. These groups probably reside outside rather than inside the Rh diporphyrin cavity because the chemical shifts of the ethoxycarbonyl groups in the diporphyrin ($\delta(CO_2CH_2CH_3)$ of **2** = –0.25 ppm, $\delta(CO_2CH_2CH_3)$ of **2** = –2.10 ppm; $\delta(CO_2CH_2CH_3)$ of **3** = –0.20 ppm, $\delta(CO_2CH_2CH_3)$ of **3** = –2.06 ppm) are only slightly further upfield than those in a monomeric etioporphyrin ($\delta(CO_2CH_2CH_3)$ = 0.62 ppm; $\delta(CO_2CH_2CH_3)$ = –1.37 ppm). Even though the external axial ligand experiences mainly diamagnetic anisotropy from the adjacent proximal porphyrin ring, the other distal porphyrin macrocycle may also exert a slight ring current on that ligand. If an ethoxycarbonyl group were ligated inside of the cavity, its ^{1}H NMR signals should appear even further upfield than those of the monomeric porphyrin because the axial ligand would be strongly affected by both porphyrin ring currents.

The ^{1}H NMR spectrum of **3** indicates that the axial ethoxycarbonyl groups must be symmetric with respect to a C_2 axis and a mirror plane parallel to both porphyrin rings. Due to this symmetry, the in–out isomer may be excluded so that either the in–in or out–out isomer is the correct one of three possible

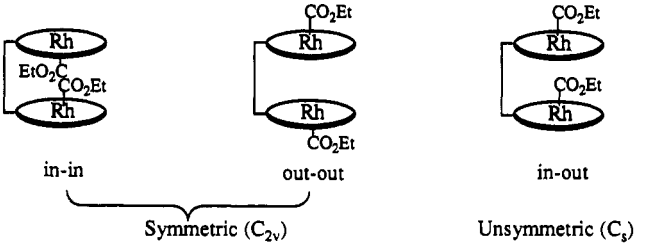

Figure 2. Possible structures of **3**.

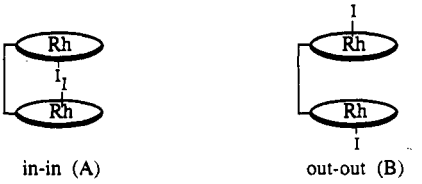

Figure 3. Possible structures of **1**.

geometric isomers (Figure 2). The ^{1}H NMR chemical shifts discussed above make the out–out isomer the most probable choice.

The diiodide complex, **1**, also exhibits an ^{1}H NMR spectrum which has C_{2v} symmetry (Figure 3). The absolute positions of axially ligated iodides in **1**, however, are uncertain. Iodides in **1** may be bound to the rhodium center as an axial ligand located inside (Figure 3A) or outside (Figure 3B) of DPB.

On the other hand, the complex, **2**, has one CO_2Et group and one iodide as axial ligands and consequently displays a ^{1}H NMR spectrum consistent with C_s symmetry. Thus, the geometric configuration of **2** is not immediately obvious because either possible configuration would have C_s symmetry. X-ray crystallography is the only way to determine the position of the iodide ligand. Though compounds **1** and **2** can be crystallized from CH_2Cl_2/CH_3OH, attempts to grow single crystals have not been successful so far. Furthermore, these compounds decompose in organic solvents within a few days and on silica over a period of hours. Fast workup and rapid column chromatography on silica gel using toluene are required to obtain the above products cleanly.

Determination of Rhodium Insertion Product Geometries. The position of the original axial groups may be inferred by the addition of PEt_3 to **1**–**3**, respectively (eqs 2–4). No adduct formation

$$Rh_2(CO_2Et)_2DPB\ (\mathbf{3}) + PEt_3 \rightarrow \text{no reaction} \quad (2)$$

$$Rh_2(I)_2DPB\ (\mathbf{1}) + PEt_3 \rightarrow Rh_2(I)_2(PEt_3)_2DPB \quad (3)$$

$$Rh_2(CO_2Et)(I)DPB\ (\mathbf{2}) + PEt_3 \rightarrow Rh_2(CO_2Et)(I)(PEt_3)_2DPB \quad (4)$$

occurs between PEt_3 and the coordinatively unsaturated diethoxycarbonyl complex (**3**) even when excess PEt_3 is used, whereas the corresponding monomeric Rh(TTP)(CO_2Et)(TTP = tetra-*meso*-*p*-tolylporphyrin) undergoes coordination of PEt_3 trans to the ethoxycarbonyl group.[14] If the axial ethoxycarbonyl groups are coordinated inside, PEt_3 should be able to ligate to Rh outside of the cavity easily. Two bulky PEt_3 ligands may not be able to enter the intraporphyrin cavity of DPB. Thus, ethoxycarbonyl groups are probably located on the outer faces of DPB.

Addition of PEt_3 to the diiodide complex (**1**) results in PEt_3 coordination outside, on the basis of the chemical shifts of coordinated PEt_3 in the ^{1}H NMR, to give a complex with C_{2v} symmetry. This indicates either that the iodide ligands are placed inside trans to the coming PEt_3 ligand (Figure 4A) or that the iodides bound outside are displaced by the PEt_3 ligands yielding

(10) Collman, J. P.; Hegedus, L. S.; Norton, J. R.; Finke, R. G. *Principles and Applications of Organotransition Metal Chemistry*, 2nd ed.; University Science Books: Mill Valley, CA, 1987; p 107.
(11) Abeysekera, A. M.; Grigg, R.; Trocha-grimshaw, J.; Viswanatha, V. *J. Chem. Soc., Perkin Trans. 2* **1977**, 1395–1403.
(12) Cohen, I. A.; Chow, B. C. *Inorg. Chem.* **1974**, *13*, 488–489.
(13) Pavia, D. L.; Lampman, G. M.; Kriz, G. S., Jr. *Introduction to Spectroscopy*; Saunders College Publishing: Philadelphia, PA, 1979; p 26.
(14) Rh(TTP)(CO_2Et)(PEt_3) ^{1}H NMR (C_6D_6, ppm): $CO_2CH_2CH_3$ obscured by a free PEt_3 proton resonances; $CO_2CH_2CH_3$ –0.84 (t, 3H); $P(CH_2CH_3)_3$ –1.49 (m (br), 9H); $P(CH_2CH_3)_3$ –2.49 (m (br), 6H).

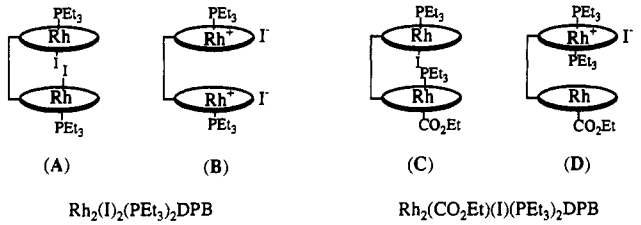

Figure 4. Suggested structures of PEt_3 derivatives of the dirhodium(III) diporphyrins, **1** and **2**.

ionic pairs (Figure 4B); the latter structure seems unlikely, but it could rearrange to the structure shown in Figure 4A.

In the reaction of the monoiodide complex (**2**) with PEt_3, the position of the coordinated PEt_3 ligands is difficult to assign. In the ^1H NMR, one PEt_3 is shifted further upfield than the other, indicating the two PEt_3 ligands are coordinated differently.[15] Two interpretations are possible: As discussed in the reactions with **1** and **3**, one PEt_3 ligand binds outside with iodide at the trans position, and the other phosphine is coordinated inside, trans to the outside ethoxycarbonyl ligand (Figure 4C). Alternatively, two phosphine ligands might be coordinated trans to one of the rhodium metal centers (Figure 4D), similar to the monomeric porphyrin system in which the pre-existing iodide ions are displaced by two PEt_3 ligands.[16] In the latter structure, the (ethoxycarbonyl)rhodium porphyrin part would not have a trans phosphine ligand inside the cavity because the PEt_3 ligand which has already been coordinated inside to the other porphyrin fragment could prevent coordination of a second PEt_3 inside the cavity. The chemical shifts of ethoxycarbonyl group should not change with PEt_3 addition in the proposed structure D because PEt_3 is not bound trans to ethoxycarbonyl. Since ethoxycarbonyl proton resonances shift downfield [$\Delta\delta = 1.03$ ($CO_2CH_2CH_3$); $\Delta\delta = 0.82$ ($CO_2CH_2CH_3$)] upon PEt_3 addition, structure C is preferred.

Although it is not possible to assign the geometry of **1**–**3**, and their PEt_3 adducts unambiguously on the basis of the above NMR data, we suggest iodide coordinates inside and ethoxycarbonyl coordinates outside of DPB, respectively.

Rh–Rh Bond Formation in Rh_2DPB. Several methods have been developed for the formation of unbridged metal–metal single bonds between rhodium porphyrins. Photolysis[17] or thermolysis[18] of rhodium porphyrin hydrides yields the corresponding Rh–Rh porphyrin dimers. Rhodium porphyrin dimers can also be produced by exposing the hydride complex to dioxygen.[18] These rhodium porphyrin dimer syntheses require hydrides as precursors, whereas the cofacial rhodium porphyrin dimer, Rh_2DPB, does not. The metalation-insertion products, $Rh_2(CO_2Et)(I)$DPB (**2**) or $Rh_2(CO_2Et)_2$DPB (**3**), can be directly converted to Rh_2DPB (**4**) (Figure 1). Thus, irradiation of **2** or **3** in benzene under vacuum gives **4** (eq 5) directly via a two-step reaction from the

$$\underset{\text{X = CO}_2\text{Et, Y = I (2)}\\ \text{X = Y = CO}_2\text{Et (3)}}{\text{Rh}_2\text{(X)(Y)DPB}} \xrightarrow[C_6H_6]{h\nu} \text{Rh}_2\text{DPB (4)} \qquad (5)$$

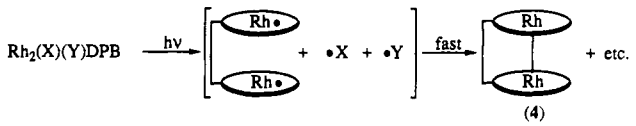

Figure 5. Synthetic pathways of Rh_2DPB (**4**) from **2** or **3** via diradicals.

free base porphyrin, whereas the preparation of either $Rh_2(OEP)_2$ (OEP = octaethylporphyrin) or $Rh_2(TPP)_2$ requires overall three steps.[18] The overall reactions are thought to occur by Rh–C and/or Rh–I homolysis, loss of the axial ligands, and combination of the two resultant Rh^{II}(Por) radicals (Figure 5). There are several precedents for this process in the context of rhodium(II) porphyrin radical formation and its dimerization.[3,6] Metal–metal bond formation occurs rather easily in the DPB system because the two porphyrin rings are preorganized for the dimerization by the biphenylene bridge. No attempt was made to characterize the volatile organic byproducts.

Rh_2DPB can also be synthesized via Rh(H)Rh(H)DPB (**5**) in three steps from the free base, H_4DPB. The diiodide complex, **1**, undergoes reduction by $NaBH_4$ presumably to the di-Rh(I) dianion, $[Rh_2DPB]^{2-}$; successive protonation of this dianionic species yields the dihydride, **5** (eq 6). The intermediate,

$$\text{Rh}_2\text{(I)}_2\text{DPB} \xrightarrow{\text{NaBH}_4} [[\text{Rh}_2\text{DPB}]^{2-}] \xrightarrow{\text{EtOH}} \text{Rh}_2\text{(H)}_2\text{DPB (5)} \qquad (6)$$

$$\text{Rh}_2\text{(H)}_2\text{DPB} \xrightarrow[C_6H_6]{O_2} \text{Rh}_2\text{DPB (4)} \qquad (7)$$

$[Rh_2DPB]^{2-}$, shows remarkable basicity. While monomeric Rh(I) porphyrin anions require a rather strong acid such as acetic acid to be protonated,[18] $[Rh_2DPB]^{2-}$ is basic enough to abstract protons from ethanol. The double negative charge may make the species more basic due to Coulombic repulsion so that protonation can occur even with weak acids. The resulting dihydride, **5**, subsequently reacts with oxygen, yielding Rh_2DPB (**4**) (eq 7) as in the synthesis of $Rh_2(OEP)_2$.

Therefore, all the rhodium insertion products we have isolated from H_4DPB can be used to form Rh_2DPB. Elemental analysis of the photolysis product, Rh_2DPB, did not give a satisfactory result probably due to some organic impurities resulting from solvent photolysis. Attempts to remove organic impurities were frustrated by decomposition during purification processes such as recrystallization or column chromatography even under an inert atmosphere.

Reactivity of Rh_2DPB with H_2 and CO. The rhodium dimer, Rh_2DPB, is completely converted to $Rh_2(H)_2$DPB in the presence of H_2 (0.5 atm) and CO (0.5 atm) at room temperature after several hours. The reaction of Rh_2DPB with H_2 and CO does not yield a metalloformyl complex[4] such as that observed in the reaction with monomeric porphyrin systems but produce a dihydride complex instead. The failure to form a formyl complex in the cofacial diporphyrin system may reflect the enhanced steric demands of CO approach to the diporphyrin cavity compared to the open site of monomeric porphyrins. In the absence of CO no reaction occurs between Rh_2DPB and H_2. Thus, we propose that H_2 approaches the inside of the Rh_2DPB cavity where the Rh–Rh bond has been weakened or broken by CO interacting on the outer faces. The intermediate radical-like Rh(II) porphyrin portions are proposed to induce homolytic cleavage of H_2 within the cavity, forming two Rh–H bonds (Figure 6). Evidence for the inner hydride formation is discussed in the following section.

Some theoretical studies on oxidative additions to dinuclear complexes[19a,b] and a review of dimetal active centers[19c] may be used to suggest a plausible pathway for this reaction. It has been

(15) $Rh_2(CO_2Et)(I)(PEt_3)_2$DPB ^1H NMR (C_6D_6, ppm): $CO_2CH_2CH_3$ 0.78 (q, 2H); $CO_2CH_2CH_3$ −1.28 (t, 3H); inner $P(CH_2CH_3)_3$ −2.04 (m, 9H), inner $P(CH_2CH_3)_3$ −3.86 (m, 6H); outer $P(CH_2CH_3)_3$ −4.87 (m, 9H), outer $P(CH_2CH_3)_3$ −7.87 (m, 6H).

(16) Upon addition of PEt_3 to Rh(OEP)(I) in CH_2Cl_2, the product displays a symmetric ^1H NMR spectrum (the methylene protons in OEP are no longer diastereotopic) containing two equivalently coordinated PEt_3 ligands; this is assigned presumably to $[Rh(OEP)(PEt_3)_2]^+(I)^-$. ^1H NMR ($CDCl_3$, ppm): H_{meso} 10.21 (s, 4H); CH_2CH_3 4.13 (q, 16H); CH_2CH_3 1.89 (t, 24H); coordinated $P(CH_2CH_3)_3$ −1.79 (m, 18H); coordinated $P(CH_2CH_3)_3$ −3.45 (m, 12H).

(17) Wayland, B. B.; Newman, A. *Inorg. Chem.* **1981**, *20*, 3093–3097.

(18) Setsune, J.-I.; Yoshida, Z.-I.; Ogoshi, H. *J. Chem. Soc., Perkin Trans. 1* **1982**, *982*–987.

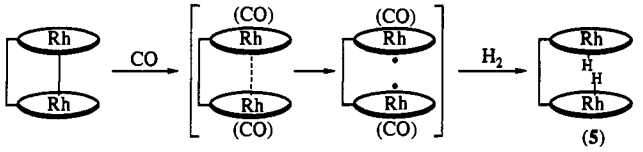

Figure 6. A suggested pathway for homolytic H_2 cleavage.

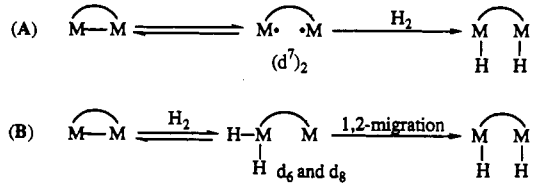

Figure 7. Possible pathways for the oxidative addition of H_2 to a dinuclear center.

suggested that the concerted addition of small molecules to dinuclear complexes involving d^7 metals such as Fe^{I}_2 or Rh^{II}_2 can occur efficiently via an intermediate diradical.[19a] Whether the reaction occurs via a synchronous concerted pathway with these diradicals $(d^7)_2$ (Figure 7A) could not be clearly demonstrated. An alternative pathway involving more than one step was also suggested. This consists of preliminary oxidative addition of a substrate to one metal and the subsequent 1,2-migration to the other metal (Figure 7B). These mechanisms avoid any termolecular step or the energetically unfavorable extraction of H• from H_2 by a single metal center. Theoretical studies favor mechanism B.[19b] However, the homolytic M–M bond rupture and subsequent M–H bond formation (mechanism A) may be possible if a facile pathway to the stable intermediate, diradical $(d^7)_2$, can be provided prior to dihydrogen addition. For example, recent studies of methane activation[3] and H_2/D_2 exchange[20] in rhodium porphyrins support the former mechanism which involves a diradical, $(Rh^{II}•)_2$.

We suggest that H_2 addition to Rh_2DPB with the help of CO also occurs via a pathway involving a diradical intermediate (mechanism A) which eventually leads to the homolytic cleavage of dihydrogen. Mechanism B is disfavored in the above reaction because cis dihydride formation is generally prohibited in metalloporphyrin systems.

The identity of the product, Rh(H)Rh(H)DPB (**5**), formed in the presence of H_2 and CO was formulated by comparing spectroscopic data of the compound derived from a completely different route. As described earlier, reduction of the diiodide complex, **1**, by $NaBH_4$ followed by protonation resulted in the formation of **5** (eq 6). The compound derived from this reaction is spectroscopically identical with the product from the reaction of Rh_2DPB with H_2 and CO. This indicates that the dihydride, **5**, from the reaction of Rh_2DPB with H_2 and CO does not contain any CO ligand because the other reaction route does not employ CO. Additionally, the absence of CO in the dihydride, **5**, derived from reaction of Rh_2DPB with H_2 and CO was verified by IR spectroscopy.

Measurements of T_1 Values of the Dihydrides. NMR spectroscopic techniques (400 MHz, 18 °C) have been employed for the further structural characterization of **5**. T_1 is defined as the characteristic time for first-order spin–lattice relaxation.[21] The T_1 value depends on the rotational correlation time, which is in turn related to the moments of inertia of the complexes studied and the viscosities of the solvents used.[22] A hydride may experience a rather fast spin–lattice relaxation (resulting in small T_1) if it interacts with hydrogens in the solvent or in other molecules which can provide a facile relaxation mechanism.

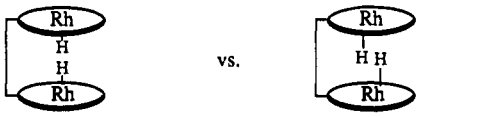

linear four-centered structure (A) side-by-side structure (B)

Figure 8. Linear four-centered vs side-by-side structure of **5**.

The hydride in monomeric Rh(OEP)(H) (OEP = octaethylporphyrin) displays an unusually small value, $(2.0 \pm 0.5) \times 10^1$ ms. In contrast, the hydrides in **5** have a remarkably high T_1 value, $(7.2 \pm 1.0) \times 10^3$ ms. Furthermore, the ^{1}H NMR spectrum of **5** exhibits a sharp doublet at –44.1 ppm ($^1J_{Rh-H}$ = 44 Hz) due to a strong ring current effect, whereas Rh(OEP)(H) displays a rather broad hydride doublet signal at –41.3 ppm with $^1J_{Rh-H}$ = 44 Hz. If **5** were the out–out isomer, the rhodium–hydride chemical shift value in **5** should be very similar to the monomeric system. Other spectroscopic properties such as the T_1 value should also be similar. The contrasting T_1 values (more than 2 orders of magnitude difference) and the different upfield hydride chemical shifts between these two compounds ($\Delta\delta$ = 2.8 ppm) indicate two different environments for the axial ligands in Rh(H)Rh(H)DPB (**5**) and in Rh(OEP)(H).

The hydride in Rh(OEP)(H) can interact with solvents and also undergoes reaction with another hydride to form $Rh_2(OEP)_2$ and H_2. Rh(OEP)(H) may also have anisotropic motion. Thus, it is not surprising that these dynamic interactions and anisotropic motion of Rh(OEP)(H) can cause the hydride to experience a short relaxation time. This remarkably small T_1 value (20 ms) is still noteworthy because normal transition metal hydride T_1 values are >150 ms.[22b,23,24] In contrast, the hydride signal in **5** displays an extremely high T_1 value. This unusually high T_1 value is due to the lack of facile spin–lattice relaxation pathways. In many cases, the dipole–dipole interaction is the dominant relaxation mechanism.[21,22b] If the hydrides are confined between the two porphyrin rings, they would not experience extensive intermolecular relaxation with solvents or with other molecules. Even if there is any intermolecular dipole–dipole interaction mechanism which might induce a fast relaxation of the hydrides in **5**, the distance between dipoles must be very small to make the relaxation efficient. The geometry of $Rh_2(H)_2$DPB in which the hydrides are located inside is not likely to permit intermolecular interaction over a short distance, thus resulting in the extremely high T_1 value of these rhodium hydrides. Therefore, we propose **5** to be a dihydridodirhodium diporphyrin complex whose hydrides are present inside the cavity.

The possibility of intramolecular interactions between two hydrides inside should be considered because such interactions tend to lower their T_1 values against the apparent high T_1. According to the proposed inner dihydride structure, dipole–dipole interaction between the two hydrides in the proximity could provide fast spin relaxation mechanisms which would reduce their T_1 values significantly. However, this is not the case in **5**. Its extremely high T_1 value implies that a fast spin relaxation is somehow inhibited, and these hydrides do not seem to undergo dipole–dipole interaction with each other.

On the basis of the estimated bond energies for these rhodium porphyrins (Rh–H = 62 kcal/mol; Rh–Rh = 15.5 kcal/mol; H–H = 104 kcal/mol),[5] the equilibrium of two Rh(Por)(H) with $Rh_2(Por)_2$ and H_2 should be thermoneutral; however there may be a large intervening kinetic activation energy. In the ^{1}H NMR, the hydride signal of **5** appears as a sharp doublet, which implies the lack of a fast equilibrium with H_2 and Rh_2DPB at room

(19) (a) Sevin, A.; Hengtai, Y.; Chaquin, P. *J. Organomet. Chem.* **1984**, *262*, 391–405. (b) Trinquier, G.; Hoffman, R. *Organometallics* **1984**, *3*, 370–380. (c) Poilblanc, R. *Inorg. Chim. Acta* **1982**, *62*, 75–86.
(20) Wayland, B. B.; Ba, S.; Sherry, A. E. *Inorg. Chem.* **1992**, *31*, 148–150.
(21) Farrar, T. C.; Becker, E. D. *Pulse and Fourier Transform NMR*; Academic Press: New York, 1971; Chapter 4.
(22) (a) Hamilton, D. G.; Crabtree, R. H. *J. Am. Chem. Soc.* **1988**, *110*, 4126–4133. (b) Crabtree, R. H. *Acc. Chem. Res.* **1990**, *23*, 95–101.
(23) Crabtree, R. H.; Hamilton, D. G. *Adv. Organomet. Chem.* **1988**, *28*, 299–338.
(24) Cotton, F. A.; Luck, R. L.; Root, D. R.; Walton, R. A. *Inorg. Chem.* **1990**, *29*, 43–47.

Table I. Hydride Characteristics of Cofacial Rhodium Porphyrin–Phosphine (or –Phosphite) Systems

	hydrides		
	$Rh_2(H)_2(PPh_3)_2DPB$	$Rh_2(H)_2(PEt_3)_2DPB$	$Rh_2(H)_2(P(OPh)_3)_2DPB$
chem shift (ppm)	−20.3	−20.1	−19.4
$^2J_{P-H}$ (t, Hz)	5	5	8
T_1 (ms)	$(1.29 \pm 0.17) \times 10^3$	$(1.39 \pm 0.08) \times 10^3$	$(1.4 \pm 0.3) \times 10^3$

temperature on the NMR time scale. Thus, the formation of H_2 and Rh_2DPB from **5** must have a large kinetic barrier, unlike the monomeric Rh(OEP)(H) system which experiences a facile equilibrium with H_2 and $[Rh(OEP)]_2$. The lack of dipole–dipole interaction or reactivity of the two inner hydrides toward the formation of Rh_2DPB and H_2 may be explained by postulating a side-by-side structure for the two inner hydrides (Figure 8B). Dihydrogen formation usually occurs via a transition state with a four-centered linear array.[3,20] If the two Rh–H bonds within the cavity exist in a rather distant side-by-side configuration instead of in a linear Rh–H- - -H–Rh structure (Figure 8A), facile dihydrogen elimination and dipole–dipole interaction may be impeded. The problem could only be resolved by X-ray crystallography followed by neutron diffraction; such a structural analysis might clarify this kinetic dilemma. However, we have been unable to grow single crystals of **5**. Thus, in the absence of additional evidence further discussion of these arguments is not appropriate.

Reactivities of Rh_2DPB with H_2 and Other Ancillary Ligands: T_1 and J_{HD} of the Resulting Hydrides. To investigate further the cleavage of dihydrogen in the cofacial Rh_2DPB system, other auxiliary ligands such as phosphines and phosphites were employed. Triphenylphosphine, PPh_3, and triethylphosphine, PEt_3, were used as ancillary ligands because these ligands are expected to weaken the Rh–Rh bond in the reaction with Rh_2DPB and H_2. Unexpectedly, reactions of Rh_2DPB with H_2 in the presence of phosphines display results different from those with H_2 and CO. In the ^1H NMR, the reaction products show a triplet at −20 ppm for the hydride ligands (J = 5 Hz in both PPh_3 and PEt_3 systems).

Whether the hydride coupling is caused by the phosphine or rhodium centers could, in principle, be determined by observing hydrogen-coupled phosphorus resonances in ^{31}P NMR. However, these measurements were hampered by sensitivity problems associated with ^{31}P NMR because of the limited quantity and the relatively low solubility of the compounds above. Instead, the origin of the coupling in the hydride triplet was investigated by employing a ligand analogous to phosphines. When $AsPh_3$ is used instead of PPh_3, the resulting hydrides display a singlet at −20.4 ppm. Thus, we conclude that the triplet originates from coupling with phosphorous, not rhodium. Since ^{31}P has a spin $^1/_2$, two phosphine ligands are required to produce a hydride triplet. Furthermore, both phosphines are required to influence the hydrides in the same manner. Rh–H coupling has not been detected within the limit of resolution. Lowering the temperature (−77 °C) did not help to detect Rh–H coupling, either. Since the magnetic moment of Rh is very small compared to that of P,[25] J_{Rh-H} tends to be much smaller than J_{P-H}, as also shown in the reaction of Rh(OEP)(H) with PPh_3 in a separate experiment [$^1J_{Rh-H}$ (24 Hz) is about 1 order of magnitude smaller than $^2J_{P-H}$ (258 Hz) at −71 °C]. Thus, it is not surprising that $^1J_{Rh-H}$ is not observed in these hydrides, considering that $^2J_{P-H}$ is less than 10 Hz.

The integration of ^1H NMR signals shows approximately two hydrogens (2H) per Rh_2DPB–bis(phosphine) adduct. The hydrides are stable only under positive pressure of H_2 (1 atm). Degassing of the solution causes the hydride signal to disappear; these hydrides slowly convert to Rh_2DPB–bis(phosphine) adducts. Reapplication of H_2 to this solution regenerates the hydride signal within several hours. This result suggests that a slow equilibrium exists between the hydrides and the Rh_2DPB–bis(phosphine) adduct under H_2.

The triplet exhibits a rather high T_1 value [T_1 (with PPh_3) = $(1.29 \pm 0.17) \times 10^3$ ms; T_1 (with PEt_3) = $(1.39 \pm 0.08) \times 10^3$ ms]. The reaction of triphenyl phosphite, $P(OPh)_3$, with Rh_2DPB and H_2 gave similar results, displaying a triplet ($^2J_{P-H}$ = 8 Hz) at −19.4 ppm with a T_1 value of $(1.4 \pm 0.3) \times 10^3$ ms. Overall characteristics of the resulting hydrides are listed in Table I. HD was employed to discern whether or not these upfield signals originated from a dihydrogen complex which might have formed in the reaction. However, no HD coupling (J_{HD} < 2 Hz in the detection limit) was observed. In addition, the high T_1 values ($>1.0 \times 10^3$ ms) also exclude the possibility of a dihydrogen complex.[26]

A dihydride structure in which each hydride is trans to the phosphines or phosphites is not likely because of the very small coupling constant between phosphorous and hydrogen. By comparison, the addition of PPh_3 to Rh(OEP)(H) at −71 °C yields a well-resolved hydride signal at −30.0 ppm as a doublet of doublets ($^1J_{Rh-H}$ = 24 Hz; $^2J_{P(trans)-H}$ = 258 Hz (*vide supra*)), even though the ^1H NMR spectrum at room temperature is so broadened that it hampers the detection of hydride signals and the measurement of coupling constants. In addition, the hydride signal in the Rh_2DPB system appears as a triplet, requiring that two phosphines influence the hydrides equally. Thus, the small P–H coupling constant, the chemical shift, and the P–H coupling of the hydrides in the Rh_2DPB–phosphine system contrasts with that observed in Rh(OEP)(H)(PPh_3). On the other hand, $^2J_{P(cis)-H}$ values have been reported in several dinuclear rhodium systems with chelated diphosphines.[27] The data on three-center two-electron bridged hydrides in these complexes shows that $^2J_{P(cis)-H}$ is usually between 4 and 13 Hz whereas $^2J_{P(trans)-H}$ is more than 50 Hz. The $^2J_{P(cis)-H}$ data from these bridged hydrides are comparable to those we have measured in hydrides of Rh_2DPB with phosphines or phosphites. However, cis phosphine–hydride orientation is very unlikely in the metalloporphyrin systems due to the steric demands of bulky phosphines. Furthermore, the observed symmetries of the two porphyrin rings resulting in a triplet for the hydrides is further inconsistent with cis phosphine–hydride arrangement.

Instead, we tentatively assign the upfield signal around −20 ppm as resulting from three-center two-electron bridged dihydrides with phosphines or phosphites coordinated outside the cavity (Figure 9). These suggested hydride structures are based on the upfield chemical shifts, large T_1 values, the absence of $^1J_{HD}$, small $^2J_{P-H}$ coupling constants, and the triplet character of this coupling. Small $^2J_{P-H}$ values may be expected in these systems because the hydrides should experience less interaction with the phosphines due to the weak through-bond interaction. The structure of inner-bridged hydrides can also explain the rather large T_1 values, in which intermolecular dipole–dipole interactions are prohibited. Intramolecular dipole–dipole interactions between suggested inner dihydrides could have lowered the T_1 values. However, measured T_1 values are large. We do not have a clear explanation for the absence of their interactions with each other, but two bridged hydrides in the molecule must not be located close enough in proximity to induce fast dipole–dipole relaxation. A large single crystal for neutron diffraction study would be required to

(25) Drago, R. S. *Physical Methods in Chemistry*; Saunders College Publishing: San Francisco, CA, 1977.

(26) Kubas, G. J. *Acc. Chem. Res.* **1988**, *21*, 120–128.

(27) Fryzuk, M. D.; Piers, W. E. *Organometallics* **1990**, *9*, 986–998.

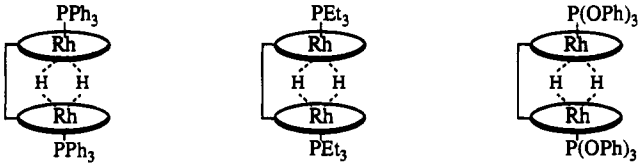

Figure 9. Three-center two-electron bridged dihydride structures suggested for the cofacial rhodium porphyrin systems with H_2 and phosphines or phosphites.

corroborate the suggested structures in which hydrides exhibit three-center two-electron bonds inside the cavity. However, our attempts to grow single crystals have been hampered by instability of these compounds over a period of hours and by the limited quantity of these compounds.

Conclusion

A novel synthesis of a cofacial dirhodium diporphyrin, Rh_2DPB (**4**), has been developed. Photolysis of rhodium insertion products, **2** and **3**, provides a convenient two-step synthesis of the cofacial diporphyrin complex **4** containing a Rh–Rh single bond. This synthesis is shortened by one step from the typical three-step synthesis of rhodium porphyrin dimers. The original three-step synthesis of metal–metal bonded **4** via the dihydride, Rh(H)Rh(H)DPB (**5**), was also carried out to confirm that the photolysis product derived from **2** or **3** is, in fact, Rh_2DPB. The reactivity of **4** with H_2 and CO was investigated. This reaction yielded Rh(H)Rh(H)DPB (**5**) in which the hydrides are probably located inside of the Rh_2DPB structure. The reaction presumably occurs via homolytic cleavage of H_2 within the cavity of Rh_2DPB where the Rh–Rh bond had been already weakened or broken by external CO. Different reactivities were discovered when phosphines or phosphites were employed as auxiliary ligands to activate the Rh–Rh bond. Spectroscopic data are consistent with three-center two-electron bonds between rhodium and hydrogen with phosphines or phosphites coordinated outside. As shown here, dinuclear centers provide methods for coordinating and/or activating molecules in the presence of ancillary ligands. Complexes derived from this dinuclear system constitute additional models for understanding reactivity observed at metal surfaces, in homogeneous catalysis, and in clusters.

Experimental Section

Standard reagents were purchased and used as received. All solvents were of reagent grade and were used without further purification except as noted below. Fresh toluene and benzene were distilled from sodium benzophenone ketyl under inert atmosphere. $[Rh(CO)_2Cl]_2$ was prepared as described in the literature procedure[7] with an extra purification by sublimation. H_4DPB was synthesized according to literature procedures.[28]

^{1}H NMR Spectra were obtained with a Nicolet NMC-300 MHz spectrometer, a Varian XL-400 MHz instrument, and a GEM-200 MHz instrument. All chemical shifts are reported in units of δ (downfield from tetramethylsilane) but were measured relative to residual ^{1}H resonances in deuterated solvents: $CHCl_3$ (7.26), C_6D_5H (7.15). UV–vis electronic absorption spectra were obtained with a Varian Cary 219 spectrophotometer or a Hewlett Packard 8450A diode array Spectrometer. Mass spectra for air stable complexes were obtained by the LSI ionization technique from the Mass Spectrometry Facility of the University of California, San Francisco, CA.

Manipulations of oxygen- and water-sensitive compounds were performed in a Vacuum/Atmospheres Co. nitrogen atmosphere drybox ($O_2 \leq 2$ ppm), on a vacuum line, or in Schlenkware flasks equipped with E. J. Young valves and O-ring vacuum adapter fittings.

$[Rh(CO)_2Cl]_2$. A 1-g amount of $RhCl_3 \cdot xH_2O$ was placed on a glass frit inside a small sublimator. Carbon monoxide was supplied to the sublimator, after being passed through an ethanol bubbler. The reaction vessel was immersed in a silicon oil bath and heated at 110 °C. Heating was continued for 24 h with a continuous CO supply; orange-red needle shaped crystals sublimed onto the sublimator wall. The first batch of these crystals was collected, while the residual crystals on the frit were extracted with *n*-hexane and the solvent was evaporated. The above two batches were combined, rapidly dried under vacuum, and kept under 1 atm of CO pressure until used.

Rh_2I_2DPB (1), $Rh_2(CO_2Et)(I)$DPB (2), and $Rh_2(CO_2Et)_2$DPB (3). The cofacial free base porphyrin, H_4DPB (20 mg, 0.018 mmol), was placed in a 50-mL round-bottomed flask containing a stir bar. Anhydrous sodium acetate (25 mg) was added, and $CHCl_3$ (25 mL) was used to dissolve the free base porphyrin. Excess $[Rh(CO)_2Cl]_2$ (30–40 mg, 0.077–0.103 mmol) was added, and the solution was stirred for 7 h. A TLC (SiO_2, 5% CH_3OH in toluene) showed two green spots. Iodine (30 mg, 0.118 mmol) was added to the stirred solution, and the resulting solution was stirred (3–8 h). The solution color changed from dark green to red black. TLC (SiO_2, 3% CH_3OH in toluene) showed that completion of the oxidation by I_2 and displayed more than three bands. The solution was transferred to a separatory funnel containing a solution of HI (0.4 mL, 47%) in water (25 mL). The organic layer was recovered and washed with saturated aqueous NaI. The organic layer was dried with anhydrous Na_2CO_3, and the solvent was evaporated. TLC (SiO_2, toluene) showed several bands. Flash column chromatography (SiO_2, toluene) gave three identifiable products, **1**–**3**, which were eluted in numerical order. These compounds were characterized by ^{1}H NMR, UV–vis, IR, and MS. The iodide-containing compounds, **1** and **2**, were recrystallized from CH_3OH/CH_2Cl_2. Yields varied among **1**–**3** (overall 30–60%), depending upon the purities of $[Rh(CO)_2Cl]_2$ and reagents.

Rh_2I_2DPB (1). ^{1}H NMR (C_6D_6, ppm): H_{meso} 9.24 (s, 2H), 9.08 (s, 4H); $H_{biphenylene}$ 6.89 (d, 2H), 6.62 (t, 2H), 6.56 (d, 2H); CH_2CH_3 4.07 (m, 8H), 3.75 (m, 4H), 3.62 (m, 4H); CH_3 3.21, 3.19 (s, 12H); CH_2CH_3 1.68, 1.46 (t, 12H, J = 7.2 Hz). UV–vis (toluene, λ_{max} (nm)): 398 (Soret), 520, 550. LSIMS: m/e = 1307, cluster, $M^+ - 2I$. Anal. Calc for $C_{76}H_{78}N_8ORh_2I_2$ (RH_2I_2DPB·H_2O): C, 57.80; H, 4.98; N, 7.09; I, 16.07. Found: C, 57.68; H, 4.92; N, 6.74; I, 16.31.

$Rh_2(CO_2Et)(I)$DPB (2). ^{1}H NMR (C_6D_6, ppm): H_{meso} 9.35 (s, 1H), 9.08 (s, 1H), 8.99 (s, 2H), 8.92 (s, 2H); $H_{biphenylene}$ 6.91 (d,d overlapped, 2H total), 6.73 (t,d overlapped, 2H total), 6.59 (t, 1H), 6.50 (d, 1H); CH_2CH_3 4.20–4.00 (m overlapped, 8H), 3.85–3.70 (m overlapped, 4H), 3.62 (m, 4H); CH_3 3.23 (s, 6H), 3.20 (s, s overlapped, 12H), 3.18 (s, 6H); CH_2CH_3 1.76 (t, 6H), 1.67 (t, 6H), 1.48 (t, t overlapped, 12H total); $CO_2CH_2CH_3$ –0.25 (q, 2H, 6.8 Hz); $CO_2CH_2CH_3$ –2.10 (t, 3H, 6.8 Hz). UV–vis (toluene, λ_{max} (nm)): 384 (Soret), 522, 553. IR (cm^{-1}): 1691 (C=O), 1061 (C–O). LSIMS: m/e = 1380, cluster, $M^+ - I$; 1307, cluster, $M^+ - I - CO_2CH_2CH_3$.

$Rh_2(CO_2Et)_2$DPB (3). ^{1}H NMR (C_6D_6, ppm): H_{meso} 9.12 (s, 2H), 8.81 (s, 4H); $H_{biphenylene}$ 6.92 (2H), 6.69 (4H overlapped); CH_2CH_3 4.15, 4.00, 3.80, 3.61 (m, 4H each); CH_3 3.23, 3.20 (s, 12H each); CH_2CH_3 1.74, 1.49 (t, 12H, each 7.4 Hz); $CO_2CH_2CH_3$ –0.21 (q, 4H, 7 Hz); $CO_2CH_2CH_3$ –2.05 (t, 6H, 7 Hz). UV–vis (toluene, λ_{max} (nm)): 388 (Soret), 524, 554. IR (cm^{-1}): 1687 (C=O), 1075 (C–O). LSIMS: m/e = 1453, cluster, M^+; 1380, cluster, $M^+ - CO_2CH_2CH_3$; 1307, cluster, $M^+ - 2CO_2CH_2CH_3$.

Rh_2DPB (4). The three products synthesized above yielded Rh_2DPB by employing the methods described below. Compound **1** (10 mg) was brought into the drybox and dissolved in THF (4 mL) and C_2H_5OH (3 mL). Excess $NaBH_4$ (5 mg) was added to the stirred solution. The solution color changed immediately from dark red to bright red. The resulting solution was stirred for 2 h, and the solvent was evaporated. The solid was dissolved in toluene and filtered through a glass wool plug to remove undissolved sodium salts. The filtrate was evaporated and dried under vacuum. A ^{1}H NMR sample was prepared in C_6D_6 in the drybox. This procedure yielded $Rh_2(H)_2$DPB (**5**). ^{1}H NMR (C_6D_6, ppm): H_{meso} 9.12 (s, 2H), 8.81 (s, 4H); $H_{biphenylene}$ 6.90 (d, 2H), 6.67 (t, 2H), 6.48 (d, 2H); CH_2CH_3 4.14, 4.01, 3.75, 3.58 (m, 4H each); CH_3 3.23, 3.14 (s, 12H each); CH_2CH_3 1.66, 1.45 (t, 12H each, 6.6 Hz); Rh–H –44.1 (d, 2H, $^1J_{Rh-H}$ = 44 Hz). UV–vis (toluene, λ_{max} (nm)): 382 (Soret), 521, 551. IR: no ν(C=O) observed.

The ^{1}H NMR sample was exposed to air. The solution color quickly changed from bright red to dark green brown. After the sample was exposed to air for several hours, the ^{1}H NMR was checked. Rh_2DPB was present; its spectrum was identical with those of Rh_2DPB formed from the other precursors, **2** and **3**, via different synthetic routes as described below. Compound **4** could be also prepared quantitatively on a bulk scale by allowing **5** to come into contact with air. Data Rh_2DPB (4) are as follows. ^{1}H NMR (C_6D_6, ppm): H_{meso} 9.36 (s, 2H), 9.25 (s,

(28) (a) Chang, C. K.; Abdalmuhdi, I. *Angew. Chem., Int. Ed. Engl.* **1984**, *23*, 164–165. (b) Collman, J. P.; Hutchison, J. E.; Lopez, M. A.; Tabard, A.; Guilard, R.; Seok, W. K.; Ibers, J. A.; L'Her, M. *J. Am. Chem. Soc.* **1992**, *114*, 9869–9877.

4H); $H_{biphenylene}$ 7.07 (d, 2H), 6.61 (t, 2H), 6.58 (d, 2H); CH_2CH_3 4.30, 3.85 (m, 8H each); CH_3 3.54, 3.29 (s, 12H each); CH_2CH_3 1.66, 1.52 (t, 12H each, 7.5 Hz). UV–vis (toluene, λ_{max} (nm)): 378 (Soret), 498 (sh), 524, 552. LSIMS: m/e = 1307, cluster, M^+.

Compound **2** (20 mg) was dissolved in dry benzene (30 mL) in a Schlenk flask equipped with an E. J. Young Teflon valve and an O-ring vacuum adapter fitting. The solution was degassed by three successive freeze–pump–thaw cycles (10^{-2} Torr). The solution was irradiated with a Hanovia mercury arc lamp for 16 h. During this time, the solution was freeze–pump–thawed twice and the irradiation was continued. The solution was evaporated and the resulting red brown solid was dried under vacuum, producing Rh_2DPB (**4**) having the same spectral data as described above.

Compound **3** (20 mg) also yielded Rh_2DPB via the same procedure as the Rh_2DPB synthesis from **2** described above. The irradiation of a degassed solution of **3** in benzene and subsequent solvent evaporation gave Rh_2DPB (**4**) as a dark brown solid. Spectral data were the same as described above.

Acknowledgment. We thank the National Science Foundation (Grant CHE9123187) for financial support. We thank Dr. Erich Uffelman for his help in the preparation of this paper. Measurement of mass spectra by the Mass Spectrometry Facility of the University of California, San Francisco, CA, is acknowledged. Y.H.'s portion of this work is dedicated to her parents (Prof. Y. G. Ha and K. S. Lee) on the occasion of her father's 60th birthday.